Rare Metal Materials and Engineering
Volume 45, Issue 7, July 2016
Online English edition of the Chinese language journal

Available online at www.sciencedirect.com
ScienceDirect

Cite this article as: Rare Metal Materials and Engineering, 2016, 45(7): 1647-1653.

ARTICLE

Hot Working Parameters Optimization of TC4-DT Titanium Alloy Based on Processing Maps Considering True Strain

Liu Jianglin[1], Zeng Weidong[1], Shu Ying[2], Xie Yingjie[2], Yang Jianchao[2]

[1] State Key Laboratory of Solidification Processing, Northwestern Polytechnical University, Xi'an 710072, China; [2] Western Titanium Technologies Co. Ltd. Xi' an 710201, China

Abstract: Elevated-temperature flow behavior of TC4-DT titanium alloy was investigated by isothermal hot compression tests at strain rate from 0.01 to 10 s^{-1} and temperature of 1181~1341 K on Gleeble-3500 simulator. Three criterions including sensitive index of the strain rate (m-value), power dissipation factor (η-value) and flow instability (ξ-value) at different strains were analyzed by the principle of processing maps. As a result, the temperature at 1181~1341 K and strain rate of 0.01~0.79 s^{-1} is the optimum region in which dynamic recovery/dynamic recrystallization (DRV/DRX) occurs, and the corresponding power-dissipation efficiency is about 45%. The alloy exhibits flow instability regimes due to flow localization at higher strain rates（>1 s^{-1}）.

Key words: TC4-DT titanium alloy; hot working parameters; processing maps; microstructure

In recent years, the increasing demands of damage tolerance have been prompted with a new kind of materials based on the design of damage tolerance[1-3]. TC4-DT titanium alloy, a new alpha-beta damage tolerance titanium alloy, has been employed as a structural material for aircraft applications due to its superior fracture toughness[4-6], and its properties are equivalent to those of Ti-6Al-4V ELI. Up to now, TC4-DT titanium alloy has received increasing attention of material scientists, and it has been researched as a candidate for structure parts with an emphasis on the relationship between processing and microstructure[4]. In previous studies, the research efforts have mainly been focused on the properties, application, and microstructure of TC4-DT titanium alloy. Guo et al.[5] investigated the microstructure and mechanical properties of TC4-DT alloy after different heat treatments and found that cooling rate and aging conditions have a remarkable effect on the microstructure parameters. Meanwhile, fatigue crack propagation behavior of different microstructures in TC4-DT titanium alloy was studied by Guo et al.[7] and the results reveal that fatigue crack propagation path is zigzag and the crack tip plasticity region is bigger in lamellar microstructure compared with the bi-modal microstructure. Peng et al.[4] studied the influence of the β processing and β annealing on the tensile properties at room and high temperature as well as fracture toughness, and draw the conclusion that β annealing was preferable to β processing with regard to gaining high fracture toughness and tensile properties with a little sacrifice of plasticity.

In general, most of the above studies on the relationship between microstructure and mechanical properties of TC4-DT titanium alloy indicate that the mechanical properties are seriously dependent on the microstructure of the structural parts. Furthermore, the final microstructure is highly associated with the hot working conditions [1]. However, little work has been conducted concerning elevated deformation behavior for TC4-DT titanium alloy. Therefore, it is of great significance to study its hot deformation characteristics and optimize the hot deformation process of the alloy.

In the present study, isothermal compression of TC4-DT alloy has been conducted at four different strain rates and six deformation temperatures. Processing maps have been applied to describe the deformation mechanisms, and to optimize hot

Received date: September 05, 2015
Foundation item: Major State Basic Research Development Program of China ("973" Program) (2007CB613807); Shaanxi Province Science and Technology Integrated Innovation Engineering Project (2012KTZB01-03)
Corresponding author: Zeng Weidong, Ph. D., Professor, School of Materials Science and Engineering, Northwestern Polytechnical University, Xi'an 710072, P. R. China, Tel: 0086-29-88494298, E-mail: zengwd@nwpu.edu.cn

deformation process. The principle of this approach is the Dynamic Materials Model which were described in detail by Prasad [8]. Briefly, the processing map is constructed by superimposing the instability map on the power dissipation map in the frame of temperature and strain rate at a certain strain. It can successfully divide the plastic deformation zone into safe and unsafe domains for avoiding deformation defects. The efficiency of power dissipation (η), is given by the strain rate sensitivity parameter (m) [9]:

$$m = \frac{\dot{\varepsilon}\mathrm{d}\sigma}{\sigma\mathrm{d}\dot{\varepsilon}} = \frac{\mathrm{d}\ln\sigma}{\mathrm{d}\ln\dot{\varepsilon}} \quad (1)$$

$$\eta = \frac{2m}{m+1} \quad (2)$$

Over this frame, the flow instability can be identified by superimposing a continuum instability criterion, and it can explain severe plastic flow provided that it is established by extreme principles of irreversible thermo- dynamics as Ref. [10] and given by:

$$\xi(\dot{\varepsilon}) = \frac{\partial\ln(m/m+1)}{\partial\ln\dot{\varepsilon}} + m < 0 \quad (3)$$

where, $\xi(\dot{\varepsilon})$ is to determine instability, and $\dot{\varepsilon}$ is the strain rate. $\xi(\dot{\varepsilon}) < 0$ means metal flow into the instability area.

1 Experiment

The composition (weight percent) of as-received TC4-DT titanium alloy is listed in Table 1. The starting microstructure as shown in Fig.1 is typically equiaxed, which consists of primary α and inter-granular β with a small amount of secondary lamellar α. The β-transus temperature for this material was measured to be approximately 1261 K by means of optical metallographic.

Compression specimens of $8^{D}\times12^{H}$ mm were machined, and then hot compression tests were conducted by a Gleeble-3500 thermal simulation machine. Concentric grooves with a depth of 0.1 mm were made on the top and bottom faces of the specimen to minimize the friction. Thermal couples were welded in the middle surface of the specimens to monitor the actual temperature of the specimen. Before starting isothermal compression, all specimens were heated to the target temperature and held for 5 min to realize the homogenization of the temperature distribution. Subsequently, the compressed samples were water-quenched immediately to preserve the microstructure at elevated temperatures. Finally, deformed specimens were sectioned parallel to the compression axis and the cut surface was prepared by standard methods. Metallographic observation was carried out on an Olympus-PMG3 optical microscope.

Table 1 Chemical composition of TC4-DT titanium alloy (wt%)

Ti	Al	V	Fe	C	Si	H	O
Bal.	6.22	4.25	0.032	0.005	0.068	0.0012	0.11

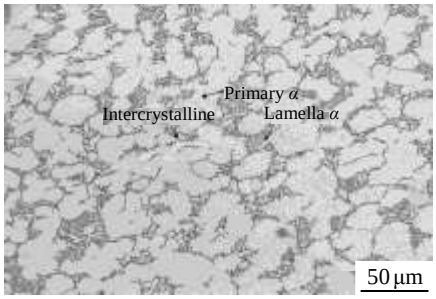

Fig.1 Microstructure of as-received TC4-DT alloy

2 Results and Discussion

2.1 Hot deformation behavior

The tests matrix was composed of constant strain rates of 0.01, 0.1, 1 and 10 s^{-1} and the deformation temperatures of 1181, 1211, 1241, 1281 and 1311 K. The true strain-true stress curves can be obtained by the load-stroke data using standard procedure. Typical flow stress curves are obtained covering single phase and dual phase regions. The characteristics of the flow curves presented by the material at different strain rates and deformation temperatures can be obviously divided into three categories, and representative curves of these features are shown in Fig.2.

(1) In the single phase region, flat true strain-true stress curves are achieved at the strain rates of 0.01~10 s^{-1}, which indicate a steady state flow behavior. Such steady-state curves present that the mechanism of work hardening is balanced by the rate of softening which may be induced by the mechanisms like dynamic recrystallization (DRX), dynamic recovery (DRV), or super plastic (SP) occurring at very high rates [11].

(2) In the dual phase region, a continuous flow softening can be observed after a peak stress at all strain rates. When a large strain arrives, these true strain-true stress curves become asymptotic and tend to reach steady state. Such a feature may be attributed to kink of lamellar structures, deformation heating, and flow instability due to flow localization or micro-cracking during deformation [1].

(3) A sudden decrease in the strain-stress curves can be found at strain rates higher than 0.1 s^{-1} through all deformation temperatures, and wide oscillations/hardening were recorded. These phenomena indicate the existence of flow localization or unsteady plastic flow of the material [12].

2.2 Hot processing map analysis

As stated before, the processing maps were established by the superposition of power dissipation maps and instability maps. They are all closely related to the strain, deformation temperature and strain rate [4]. Table 2 listed the flow stress under different strain rates, and deformation temperatures when the strain is 0.5. The detailed procedure of processing maps at this strain is as follows.

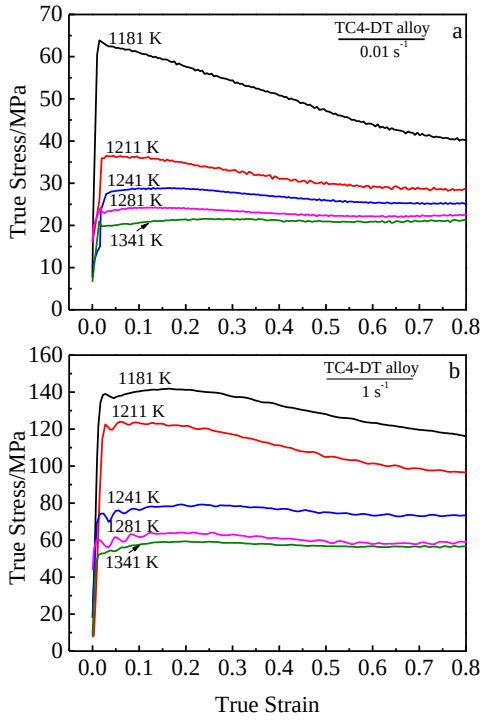

Fig.2 True stress-strain curves of TC4-DT titanium alloy at various deformation temperatures with strain rate of 0.01 s^{-1} (a) and 1 s^{-1} (b)

Table 2 Flow stress values of TC4-DT alloy at different deformation temperatures, strain rates when strain is 0.5 (MPa)

Strain rate/s^{-1}	Deformation temperature/K					
	1181	1211	1241	1281	1311	1341
0.01	47.08	30.25	25.91	22.45	20.93	19.51
0.1	79.21	58.63	48.45	34.98	33.24	31.58
1	128.03	104.91	75.04	59.33	56.69	54.17
10	202.91	146.51	117.45	95.18	83.15	72.64

When the strain is 0.5, the relationship between $\ln\sigma$ and $\ln\dot{\varepsilon}$ at different deformation temperatures are shown in Fig.3, which presents that flow stress and strain rate have a good linear relationship, and the material meet the hypothesis of DMM [13].

The strain rate sensitive index '*m*' is calculated by Eq.(1). Fig.4 shows the 3D response surface. It indicates that the change tendency of *m*-value with deformation temperature and strain rate is similar at different strains. However, strong waves indicate that the deformation mechanism of work-piece has been changed violently. Microstructure changes at different temperatures need so much heat dissipation that *m*-values increase greatly. The microstructure defects appear when $m<0$, and defects are identified by the combination of power dissipation map and instability map.

The number of contour map represents power dissipation factor (η), which can be obtained by Eq.(2). It describes the

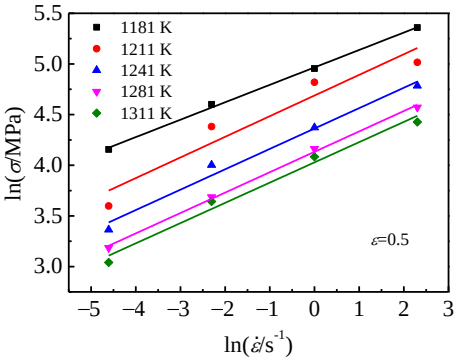

Fig.3 Linear relationships between $\ln\sigma$ and $\ln\dot{\varepsilon}$ at different deformation temperatures

relative rate of internal entropy production during hot deformation, and it also means the dissipative microstructure change under different strain rates and deformation temperatures[14]. The larger the η-value, the better the performance of formed organization. This may cause a variety of deformation mechanisms, such as DRX or DRV, and flow localization [15]. It can be seen from Fig.5 that the efficiency of power dissipation decreases with the increasing strain rates in the dual phase region, while it first increases and then decreases in the single phase region through all the strains. The same changing trend has been found by Zhu et al. [1] for TC21 alloy. In the dual phase region, three peak efficiencies of 43%, 44%, 50% and 53% appear at the tempera- ture and strain rate ranges of (i: 1193~1223 K, 0.01~0.1 s^{-1}), (ii: 1215~1246 K, 0.01~0.178 s^{-1}), (iii: 1230~1243 K, 0.01~0.015 s^{-1}) and (iv: 1227~1243 K, 0.01~0.015 s^{-1}) at the strain of 0.1, 0.3, 0.5 and 0.7, respectively. Therefore, the optimum condition for hot processing of the alloy is the region of low strain rates ($\dot{\varepsilon} < 0.1$ s^{-1}), which implies that the workability will be improved in this domain; In the single phase region, the only peak η-value appears around the deformation temperature of 1293 K and the strain rate about 0.316 s^{-1}, and the peak area gradually decreases to a point with the increase of strain. However, the high η-values do not represent the safe domain and the ξ-values must be analyzed further.

Meanwhile, Fig.5 indicates that the high efficiency domain ($\eta > 0.33$) changes with the strain, and it gradually increases with the increase of strain, and the high efficiency domain appears at the high strain rates. It is obvious that the efficiency reaches the peak values in the temperature range of 1223~1243 K, logarithm of strain rate range from −2 to 0.5. The low efficiency domains locate in the low deformation temperature, high strain rate condition. It is mainly because that the deformation time is insufficient, the DRX is difficult to occur under the low temperature and high strain rate condition, thermal activation is relatively hard to start under low temperature and not enough time to nucleate. The above analysis shows that peak efficiency of this alloy occurs in the

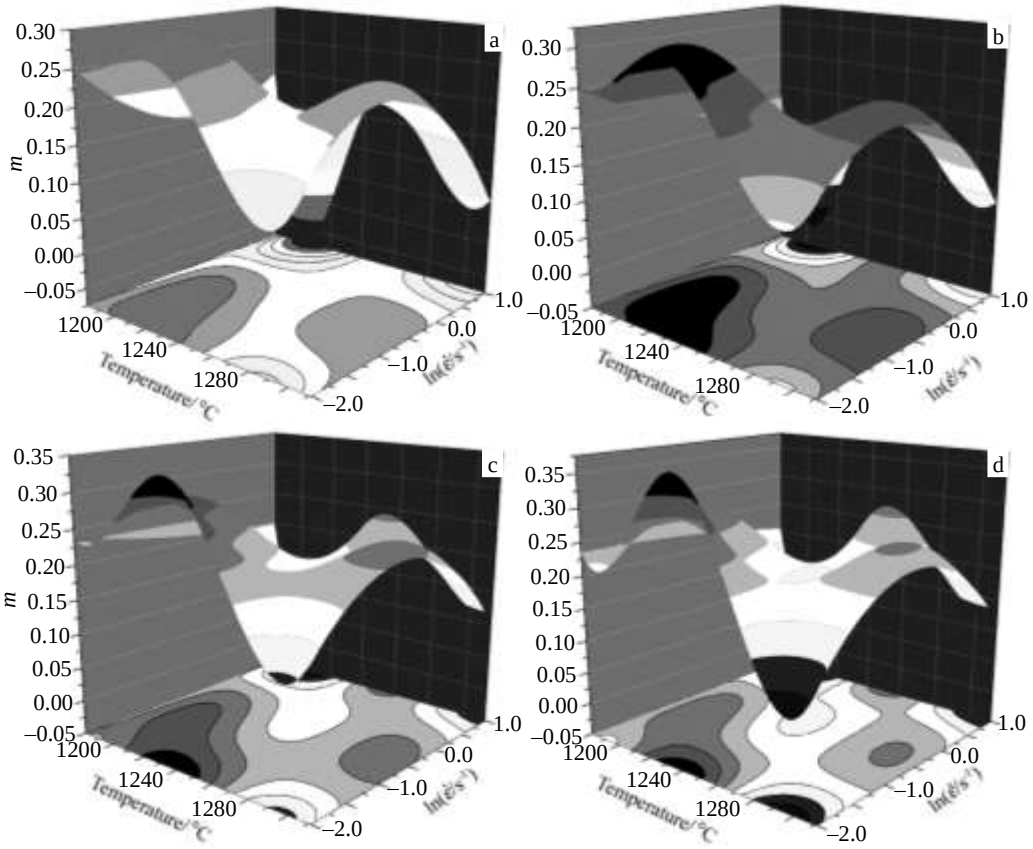

Fig.4 3D response surface of *m*-value on strain rate and deformation temperature at different strains: (a) 0.1, (b) 0.3, (c) 0.5, and (d) 0.7

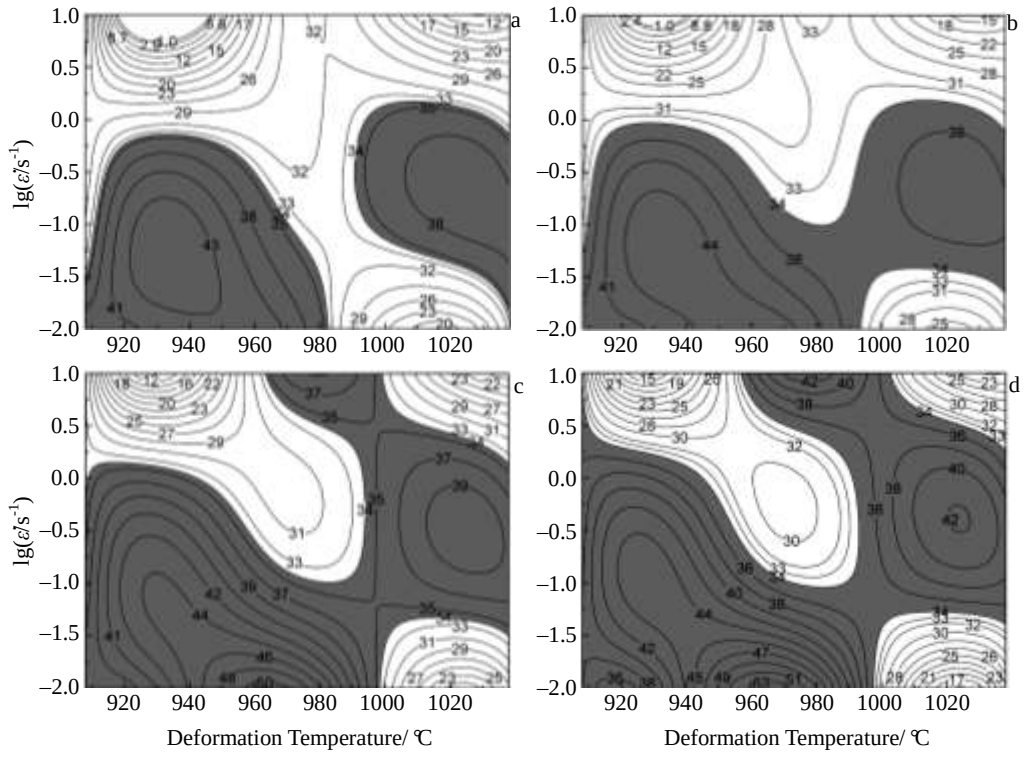

Fig.5 Processing efficiency maps at different strains: (a) 0.1, (b) 0.3, (c) 0.5, and (d) 0.7

domains: (1) In the dual phase region, the better deformation condition is 1233 K/0.01 s^{-1}; (2) In the single phase region, it goes to 1303 K/0.316 s^{-1}.

The relationship of ξ about temperature (T) and strain rate ($\dot{\varepsilon}$) can be expressed by Eq.(3), and the maps (Fig.6) can be obtained by cubic curve fitting. In the contour maps, shadow regions indicate the flow instability, and the remaining area represents flow stability. As shown in Fig.6a~6d, the flow instability region mainly locates in low and high temperature with high strain rate. In the stability domain, microstructure evolution is realized in the form of DRV and DRX, strain decreases and the unstable factors appear. In the instability domain, flow localization and crack along grain boundary appear. Along with the deformation, heterogeneous crystalline boundary leads to large deformation which results in flow instability.

As can be seen from Fig.6, there is no significant difference as regards the features about the maps developed at high strains. Some domains can be distinguished. It can be seen from Fig.6a and Fig.7a that: (1) in the temperature range of 1181~1233 K and logarithm of the strain rate range of 0.01~−0.25 s^{-1}, the peak efficiency is about 44% in Domain #1; (2) in the temperature range of 1264~1311 K and logarithm of the strain rate range of 0.01~0.084 s^{-1}, the peak efficiency is about 40% in Domain #2; (3) in the Domain #3, the stability region covers the whole experimental range of strain rate, the temperature range of 1233~1264 K, while no peak efficiency in the Domain. As shown in Fig.6b and Fig.7b: (1) in the temperature range of 1181~1233 K and logarithm of the strain rate range of 0.01~0.145 s^{-1}, the peak efficiency is about 44% in Domain #1; (2) in the temperature range of 1271~1311 K and logarithm of the strain rate range of 0.01~0.084 s^{-1}, the peak efficiency is about 39% in Domain #2; (3) in the Domain #3, the stability region covers the whole experimental range of strain rate, and the temperature range of 1233~1264 K, while no peak efficiency is found. From Fig.6c and Fig.7c: (1) in the temperature range of 1181~1223 K and logarithm of the strain rate range of 0.01~0.08 s^{-1}, the peak efficiency is about 44% in Domain #1; (2) in the temperature range of 1283~1311 K and logarithm of the strain rate range of 0.01~0.24 s^{-1}, the peak efficiency is about 39% in Domain #2; (3) in the Domain #3, the stability region covers the whole experimental range of strain rate, and the deformation temperature range of 1223~1283 K, the peak efficiency value is 50%. Compared with the first three figures, Fig.6d and Fig.7d show that the stability regions expand, especially the Domain #3, which is because two extreme efficiency values appear.

In a word, the reason why the safe domains mainly locate in the low strain rate region is that power dissipation factors will be elevated with the increase of strain rate and deformation temperature. This is also the primary cause of DRV and DRX. On the contrary, the power dissipation factors decrease with the increase of strain in low deformation temperature and high strain rate domains, and it can generate flow instability.

2.3 Microstructure evolution

To validate the analysis on distribution of power efficiency and instability/stability region of the alloy, the microstructure of the corresponding deformation conditions are presented in Fig.8.

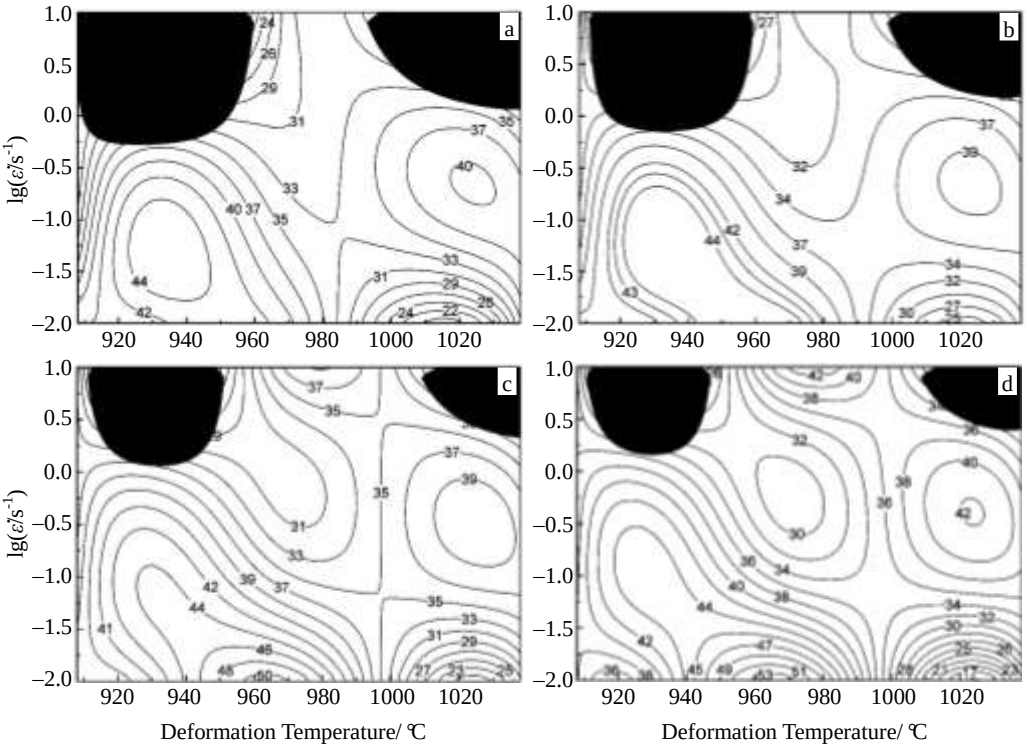

Fig.6 Instability maps of the TC4-DT titanium alloy under different strains: (a) 0.1, (b) 0.3, (c) 0.5, and (d) 0.7

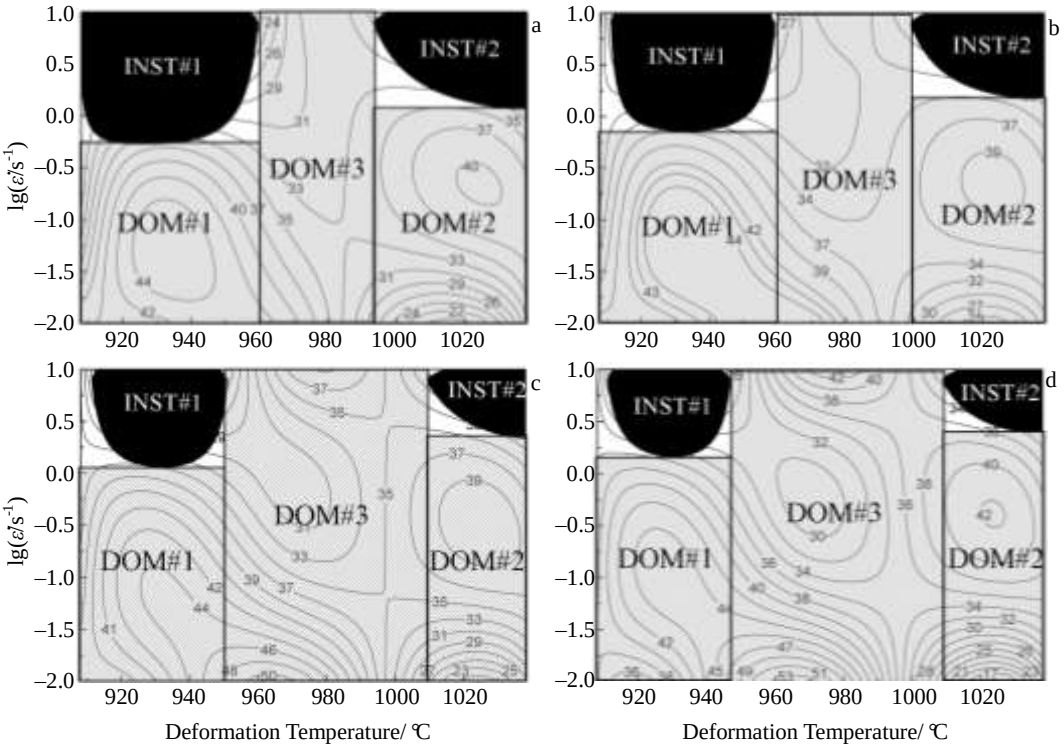

Fig.7 Processing maps of the TC4-DT titanium alloy under different strains: (a) 0.1, (b) 0.3, (c) 0.5, and (d) 0.7

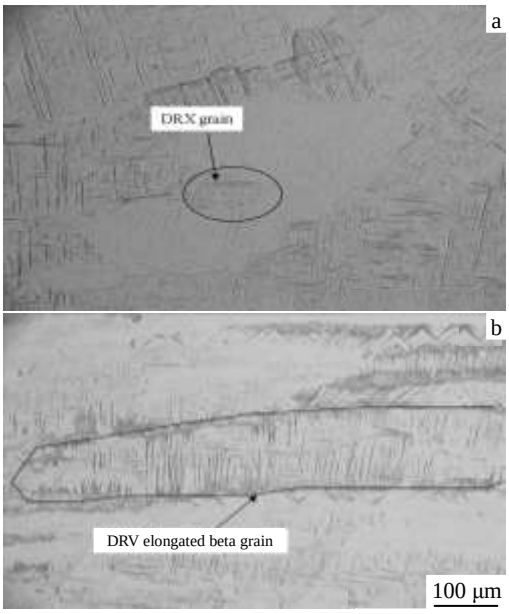

Fig.8 Optical metallographs of specimens deformed under different conditions: (a) 1311 K/0.01 s^{-1}/30% and (b) 1311 K/10 s^{-1}/70%

Generally, low η-values appear in the conditions of high strain rate, while the corresponding large values appear at low strain rate. The microstructures of specimens deform at temperature of 1311 K and strain rate of 0.01 s^{-1}, when it is 30%, and the temperature of 1281 K with strain rate of 10 s^{-1} when it is in 70%. A small quantity of recrystallization grains occurs in β grains under the former deformation condition. In addition, it can be seen from Fig.8 that the grains are elongated due to deformation, and the grain boundaries are irregular, which present typical DRV feature. Sivakesavam and Prasad[13] pointed out that the DRX may be considered to consist of two competing processes: formation of interfaces (nucleation), and migration of interfaces (growth). The nucleation consists of the formation of a grain boundary due to the dislocation generation simultaneous recovery and rearrangement. However, it is not difficult to see from Fig. 8a that there are no obvious processes for nucleation and growth occurring during deformation of TC4-DT alloy. It can be concluded that the main deformation mechanism of TC4-DT titanium alloy is DRV, and the microstructure after plastic deformation is constituted of flat elongated β grains discontinuous recrystallization grains on the grain boundary. Microstructures also confirm that steady state flow and flow softening features of true stress-strain curves display DRV and discontinuous recrystallization, respectively.

From Fig.6 and Fig.7, it can be clearly seen that the instability domains mainly occur in the region of strain rate above 1 s^{-1}, and instability domains expand with the increase of strain. The microstructure manifestation of instability regarding the present alloy has been discussed before, which corresponds to the specimen deformed at 1181 K/10 s^{-1} with deformation of 70%. The microstructure exhibits flow localization which have been associated with local

temperature rise at higher strain rates (>1 s^{-1}), because at higher strain rates, flow localization is conducted due to insufficient deformation time and low thermal conductivity of the material. It is undesirable in obtaining consistent mechanical properties and thus should be avoided during processing. However, serrate oscillation of stress-strain curves above 1 s^{-1} (Fig.3) is possibly associated with flow instability as reported in Ref. [16].

3 Conclusions

1) The true stress-strain curves of TC4-DT alloy are obtained based on isothermal compression tests of TC4-DT titanium alloy in the strain rate range from 0.01 to 10 s^{-1} and deformation temperature range of 1181~1341 K on Gleeble-3500 simulator. The hot processing maps are established by the m-value, η-value and ξ-value.

2) Microstructure at different deformation conditions and processing maps at the strain of 0.1, 0.3, 0.5 and 0.7 are used to divide the mechanism of stability and instability during deformation. DRV/DRX at large power dissipation appears at low deformation temperature and strain rate. The recrystallization also could be found in the high deformation temperature range, which is characterized by a medium of η-value.

3) The stability domain occurs in the temperature range of 1181~1341 K and strain rate range of 0.01~0.79 s^{-1}, with two domains of peak efficiency: one occurs at 1233 K/0.01 s^{-1} with a peak efficiency of about 53% that is associated with DRX; the other occurs at 1293 K and strain rate 0.79 s^{-1}, with a peak efficiency of about 42%, which displays the feature of DRV. However, at higher strain rates, the tested material undergoes flow instability manifesting as flow localization and cracking along grain boundary, which should be avoided.

References

1 Zhu Yanchun, Zeng Weidong, Feng Fei *et al*. *Materials Science and Engineering A*[J], 2011, 528(3): 1757

2 Guo Ping, Zhao Yongqing, Hong Quan *et al*. *Rare Metal Materials and Engineering*[J], 2013, 42 (11): 2367 (in Chinese)

3 Lei Jinwen, Zeng Weidong, Zhu Zhishou *et al*. *Transactions of Materials and Heat Treatment*[J], 2009, 30(5): 14 (in Chinese)

4 Peng Xiaona, Guo Hongzhen, Shi Zhifeng *et al*. *Materials Science and Engineering A*[J], 2014, 605: 80

5 Guo Ping, Zhao Yongqing, Zeng Weidon *et al*. *Materials Science and Engineering A*[J], 2013, 563: 106

6 Peng Xiaona, Guo Hongzhen, Shi Zhifeng *et al*. *Materials & Design*[J], 2013, 50: 198

7 Guo Ping, Zhao Yongqing, Hong Quan *et al*. *Rare Metal Materials and Engineering*[J], 2014, 43(6): 1479 (in Chinese)

8 Prasad Y V R K, Gegel H L, Doraivelu S M *et al*. *Metallurgical and Materials Transaction A*[J], 1984, 15(10): 1883

9 Srinivasan N, Prasad Y V R K, Rama Rao P. *Materials Science and Engineering A*[J], 2008, 476: 146

10 Prasad Y V R K. *Indian Journal of Science and Technology*[J], 1990, 28: 435

11 Liu Jianglin, Zeng Weidong, Lai Yunjin *et al*. *Materials Science and Engineering A*[J], 2014, 597: 387

12 Ma Xiong, Zeng Weidong, Wang Kaixuan *et al*. *Materials Science and Engineering A*[J], 2012, 550: 131

13 Sivakesavam O, Prasad Y V R K. *Materials Science and Engineering A*[J], 2003, 362: 118

14 Seshacharyulu T, Medeiros C S, Frazier W G *et al*. *Materials Science and Engineering A*[J], 2000, 284: 184

15 Momeni A, Dehghani K, Ebrahimi G R. *Journal of Alloys and Compounds*[J], 2011, 509(39): 9387

16 Ankem S, Shyue J G, Vijayshankar M N *et al*. *Materials Science and Engineering A*[J], 1989, 111: 5

基于应变影响热加工图的 TC4-DT 钛合金热成形工艺参数优化

刘江林[1]，曾卫东[1]，舒 滢[2]，谢英杰[2]，杨建朝[2]

(1. 西北工业大学 凝固技术国家重点实验， 陕西 西安 710072)

(2. 西部钛业有限责任公司，陕西 西安 710201)

摘 要：利用 Gleeble-3500 热模拟试验机，在变形温度为 1181~1341 K 及应变速率为 0.01~10 s^{-1} 参数范围内对 TC4-DT 钛合金进行等温恒应变速率压缩试验。基于加工图理论分析了不同应变条件下应变速率敏感因子、功率耗散因子及失稳区的区别与联系，分析加工图发现: TC4-DT 钛合金在 1181~1341 K，应变速率为 0.01~0.79 s^{-1} 之间主要发生动态再结晶/动态回复（DRV/DRX），此区间对应的能量耗散效率大致为 45%，当变形发生在温度 1181~1211 K，较高应变速率（>1 s^{-1}）下，对 TC4-DT 钛合金加工时易发生流变不稳定现象。

关键词：TC4-DT 钛合金；热加工参数；加工图；微观组织

作者简介：刘江林，男，1984 年生，博士生，西北工业大学凝固技术国家重点实验室，陕西 西安 710072，电话：029-88494298，E-mail: jlliu84@sina.com